Tuning Magnetic Anisotropy in Metallic Multilayers by Surface Charging: An *Ab Initio* Study

P. Ruiz-Díaz, T. R. Dasa, and V. S. Stepanyuk

Max-Planck-Institut für Mikrostrukturphysik Weinberg 2, D-06120 Halle, Germany

Our *ab initio* studies show clear evidence that magnetic anisotropy (MA) and the direction of magnetization in metallic magnetic multilayers can be tailored at once by surface charging. By taking Fe-Pt multilayers as a representative example, we demonstrate that surface charging has a deep effect on the magnitude of the MA, which is composition dependent, achieving remarkably large values for systems featuring a single Fe layer capped with Pt. More intriguing is the behavior of the multilayers capped with iron bilayers, for which surface charging not only affects the value of the anisotropy but an easy-axis switching is also revealed. By analyzing the electronic structure of the magnetic layers and relating the MA to the orbital moment anisotropy, some insights about the origin of the MA from a local perspective can be inferred.

The magnetic anisotropy of nanoscale systems, being one of the key parameters for spintronic data storage and processing, has recently received considerable attention from both experimental and theoretical perspectives [1–3]. Diverse ways of manipulating the electronic and magnetic properties have been sought and found. These include alloying [4], external electric field exposure [1,5–7], and electrolyte charging [7–9]. Large values of MA are often preferred in order to stabilize the orientation of the magnetization in a sample against thermal fluctuations, making the low-energy magnetization reversal processes unfeasible, however. Therefore, the hunt for a system that would exhibit large anisotropy and be easy to manipulate at the same time is still on.

Commonly, MA arises as a result of large intra-atomic spin-orbit coupling (SOC) interactions. Strong magnetic materials, $3d$ transition metals, usually display poor SOCs in contrast to their heavier counterparts ($4d$-$5d$ elements) which are paramagnetic but highly polarizable. Thus, by alloying both atomic species, a higher degree of magnetic anisotropy is often introduced [10]. This has been the most explored way to increase the robustness of MA in past years [11,12]. An external electric field (EEF) induced by the application of a voltage gate is an alternative mechanism to tune the local magnetic properties, which has been successfully investigated, particularly in ultrathin films [5,13–15] or in low-dimensional systems such as aggregates and atomic chains deposited on substrates [16]. Another promising route, widely used in electrochemistry [8,9] but less investigated in the field of spintronics, to modify and control the intrinsic mechanical [17], transport [18], electronic [19], and magnetic [20,21] properties of materials is through the change in the carrier density or charge doping. Remarkably, it has been shown that all these properties are extremely sensible to the excess of electrons (holes) and can be easily tailored. The most natural way to induce a charge (hole) injection in nanosized systems is by electrolyte charging [7,8]. Nevertheless, this method usually requires the use of liquid electrolytes to induce a change in the carrier density. Novel and more sophisticated methods of achieving local charge injection involve the use of scanning tunneling microscopy [22], scanning probe microscopy [23], and electron force microscopy tips [24].

Among all the possible $3d$-$5d$ alloys, the Fe-Pt compounds are particularly attractive for technological applications such as magnetic recording design [7]. Indeed, previous theoretical studies on Pt-Fe ultrathin films reported anisotropy energy values of ~5 meV/ magnetic atom [13]. Not only having large MA values but controlling the orientation of the magnetization would be essential for reducing the size of the magnetic storage bits. A very early study of ultrathin epitaxial Fe layers deposited on Au(001) predicted a spin reorientation from in-plane to perpendicular MA depending on the film thickness [25]. Hence, the aim of the present work is to investigate both alloying and charge-doping effects in $3d$-$5d$ layered alloys taking the Fe-Pt ultrathin films as a particular example. Our study shows that by combining both features, the magnitude of the MA and the orientation of the magnetization can be tuned at once.

Calculations have been performed within the framework of density functional theory [26] using a supercell approach as implemented in the Vienna *ab initio* simulation package (VASP) [27]. For exchange and correlation interactions, the local Ceperly-Alder functional [28] as parametrized in Ref. [29] is employed. First, scalar calculations are performed for structural optimization and then fully relativistic ones for determining the MA afterwards. Further details about the parameters used in the present calculations are summarized in Ref. [30]. The Fe-Pt multilayers on Pt(001) are modeled by a slab with 12–14 layers with ten of them representing the host Pt substrate. By means of a uniformly charged background, true surface

charging in the slabs can be simulated [31]. The charge doping is controlled by the number of valence electrons. Typically, by adding (removing) on the order of 1.2 e per unit cell to the neutral system, one can simulate a negative (positive) charge doping. Quadrupolar corrections [32] are not necessary for determining the MA [33]. The MA, taken as the energy difference between systems with the magnetization aligned along two orthogonal crystallographic axes, i.e., $E[001] - E[100]$, is obtained self-consistently. For the sake of comparison, the magnetic force theorem was used [34]. It was found that both approaches yield similar tendencies and values for the MA. Thus, only self-consistent results are discussed in the present work, although both results are shown.

The surface-charging effects on the MA in the Fe-Pt multilayers are investigated for several capping compositions. First, the charge-doping influence on the structural relaxation of the multilayers was found not to be determinant in the magnitude of the MA. The effect is a modest interlayer expansion of less than 2% leading to MA variations of less than 1%. We start our analysis by considering Pt/Fe/Pt(100), which has a relatively large MA (5.12 meV/Fe atom) and out-of-plane axis of magnetization [13]. Further, for this particular system, a change of ~13% in the MA has been predicted in the presence of an EEF [13,14]. In agreement with these previous studies, we estimated a MA value of 5.4 meV/magnetic atom for a neutral system having an out-of-plane axis of magnetization. Nevertheless, charge doping was found to have a stronger effect on the MA than an EEF. As shown in Fig. 1, a linearlike behavior [35] is found with a remarkable MA enhancement for positive charging (excess of holes) of ~50% (8.2 meV/magnetic atom for 1.2 holes/unit cell) and a considerable reduction for
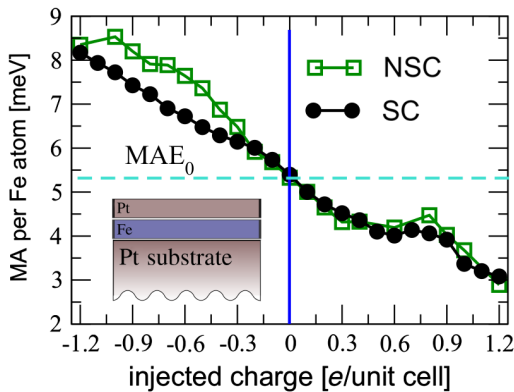

FIG. 1 (color online).   Calculated self-consistent (SC) and non-self-consistent (NSC) magnetic anisotropy energy (in meV/per magnetic atom) for Pt/Fe/Pt(001) as a function of the injected charge (holes). The charge-doping scale (in units of e/unit cell) is referred to the neutral system. Positive (negative) values stand for an excess (lack) of valence electrons. The dashed lines are only to guide the eye to find the MA in the neutral system.

negative charging (excess of electrons) of ~40% (3 meV/magnetic atom for $1.2e$) with respect to the neutral system. Therefore, the observed changes in the magnitude of the MA as a function of the charge injection constitute a net variation in the anisotropy energy ΔE of nearly ~95% (5.2 meV/magnetic atom), which is of the order of the MA for the neutral system itself.

The MA behavior seems not to be exclusive to this particular multilayer composition but quite more general. By capping the former system with a second Pt layer, i.e., Pt_2/Fe/Pt(100), or alternating the Pt-Fe layers twice, Pt/Fe/Pt/Fe/Pt(100), a similar linear dependence in the MA as a function of charge injection is found but always reaching smaller MA values (~ 2.5 meV for both neutral systems). This suggests that neither capping with a second nonmagnetic layer nor alternating magnetic layers can considerably affect the local electronic environment exhibiting the robustness of the MA against hybridizations and spin-orbit interactions. Moreover, due to the large MA, the out-of plane axis of magnetization is preserved.

More intriguing is the magnetic behavior of the Pt slabs capped with iron bilayers. We discuss two possible scenarios: when the Pt-substrate is capped with a Fe bilayer first, and then with one or two additional Pt layers obtaining Pt/Fe_2/Pt(100) and Pt_2/Fe_2/Pt(100) configurations, respectively. In contrast with the previous investigated systems, we found they display small MA values (roughly 1.4 and 0.5 meV/magnetic atom, respectively) with an in-plane axis of magnetization, making them likely candidates for developing spin reorientation if the local electronic environment is strongly modified. Moreover, the linear relationship between the MA and charge doping vanishes for both systems, showing a more complex dependence. The MA behavior as a function of the injected charge is shown in Fig. 2. The MA hardly varies for electron doping; the net changes in the MA $\Delta MA = |MA(1.2)| - |MA(0)|$, are estimated to be 1.3 and 1.8 meV/magnetic atom with respect to the neutral value for Pt/Fe_2/Pt(100) and Pt_2/Fe_2/Pt(100), respectively. However, for hole injection a considerable variation in the MA is found to follow partial linear behavior. Simultaneously, a transition in the axis of magnetization from in plane to out of plane is observed for both systems above 0.6 holes. After easy-axis switching, the MA rises to high values of ~2.5 meV/magnetic atom, indicating the stability of the magnetization reorientation. Thus, charge doping gives us the possibility of engineering capped multilayers with two stable directions of magnetization. Furthermore, from our analysis we conclude that the interaction of the double Fe layer with the capped Pt layer and the substrate is essential in the magnetization reversal. Indeed, in a more detailed investigation of similar Fe-Pt and Fe-Pd multilayers capped with two Fe layers such as Fe_2/Pt(100), Fe_2/Pd(100), Pd/Fe_2/Pd(100), and Pd_2/Fe_2/Pd(100), easy-axis switching is always observed.
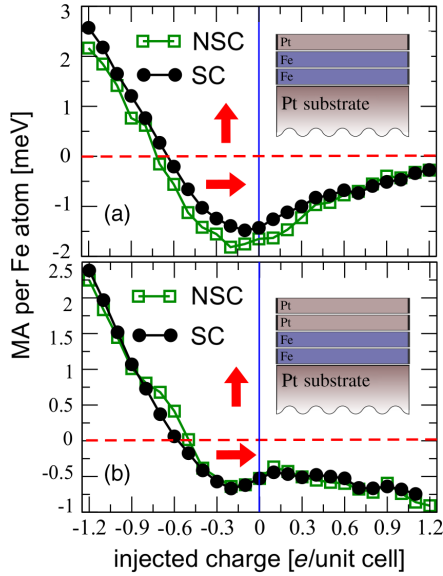
FIG. 2 (color online). Calculated self-consistent (SC) and non-self-consistent (NSC) MA per magnetic atom for (a) Pt/Fe$_2$/Pt(100) and (b) Pt$_2$/Fe$_2$/Pt(100). The charge doping (in units of e/unit cell) has the same meaning than in Fig. 1. Positive (negative) MA values stand for an out (in-plane) axis of magnetization.

In order to elucidate this intricate behavior found in the Fe-Pt multilayers, we analyze the d-orbital-resolved local density of states (LDOS) of the magnetic layer in Pt/Fe/Pt(100), which is expected to give the main contribution to the MA [13], through the well-known second-order perturbation formula [36]

$$\text{MA} = E_x - E_z \sim \xi^2 \sum_{o,u} \frac{|\langle \psi_u | l_z | \psi_o \rangle|^2 - |\langle \psi_u | l_x | \psi_o \rangle|^2}{\epsilon_u - \epsilon_o}, \quad (1)$$

where $\{\psi_o, \psi_u\}$ stand for the unoccupied (occupied) states and $\{l_x, l_z\}$ are the angular momentum operators, respectively. The ξ parameter is an average of the SOC coefficient. Clearly, the most dominant contributions to the MA come from the states near the Fermi level and its behavior is essentially determined by the denominator of Eq. (1). Further, ignoring the spin-flip terms between up and down states, as for Fe the majority d band is fully occupied, the predominant changes in the MA can be only attributed to the coupling between states in the minority band. After analyzing the spin-orbit coupling matrix elements between the different d orbitals, we found that the d_{xy} and d_{xz} orbitals have the highest contribution to the MA. These orbitals are coupled with each other through the l_x operator leading the variations in the MA to arise from the second term in Eq. (1). Insights about the nature of this coupling can be qualitatively inferred from LDOS features, which provide direct information about the local structure, particularly about the MA behavior [37]. For instance, as can be seen in Fig. 3, for hole-doping (positive charging) the
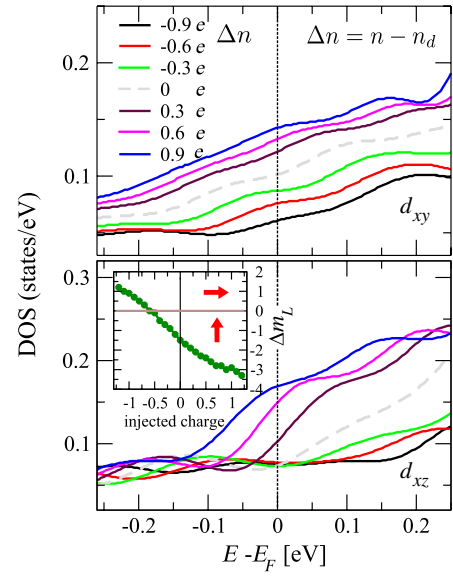

FIG. 3 (color online). Decomposed minority d-orbital local density of states (LDOS) for the Fe layer in the case of the system depicted in Fig. 1, for same representative charge-doping values, $\Delta n = n - n_d$ where $n(n_d)$ refers to the number of electrons in the charged (neutral) system, respectively. Inset: orbital moment differences ($\Delta m_L = m_L^x - m_L^z$ in units of 10^{-2} μ_B). Arrows indicate the direction of the highest orbital contribution.

d_{xz} orbitals remain unchanged, while the d_{xy} orbitals undergo a depletion near the Fermi level decreasing the spin-orbit coupling between them, and resulting in an enhancement of the MA. Such a reduction is monotonic (due to the gradual depletion of d_{xy} orbitals as the number of holes is increased) and this might explain the observed linear enhancement in the MA. On the other hand, for electron injection (negative charging), the coupling between the d_{xz} and d_{xy} orbitals rises fast increasing the SOC interaction which leads to a reduction of the MA. The analysis of explaining MA trends through the second-perturbation formula can be extended to other samples. As an example, for Pt/Fe$_2$/Pt(100), the main contribution to the MA comes from the coupling between the d_{xy} and $d_{x^2-y^2}$ orbitals. However, in this case, the coupling between the d_{yz} and $d_{x^2-y^2}$ orbitals $\langle d_{x^2-y^2} | l_x | d_{yz} \rangle$, which favors an in-plane magnetization, also has an important contribution to the MA. Therefore, the interplay between these two couplings determines the direction of the easy axis. Moreover, one can relate the MA to the orbital moment anisotropy (OMA), which is found to partially follow Bruno's relation [$\Delta E_{\text{SOC}} = -(\xi_{\text{Fe}}/4\mu_B)\Delta m_{l,\text{Fe}}$] [34], since the highest orbital moment lies in the easy axis only in the range of -0.6 to $1.2e$/unit cell (see the inset of Fig. 3).

For Pt/Fe$_2$/Pt(100) it is also possible to associate the MA with the OMA. Here, the total orbital moment of the Fe bilayer goes along with a linear dependence in the MA,
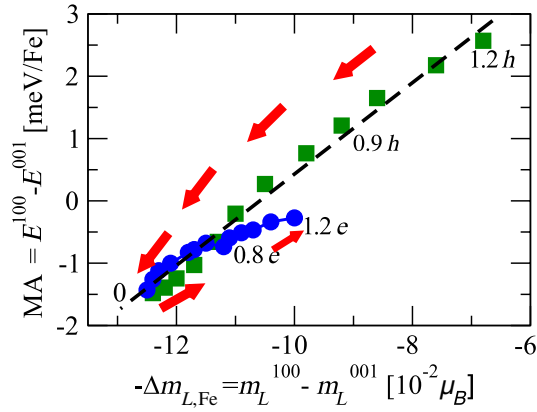
FIG. 4 (color online).   Relationship between MA and OMA of the Fe bilayer in $Pt/Fe_2/Pt(100)$. Arrows indicate the direction of the MA behavior as a function of the injected electrons (holes).

following in part Bruno's criterion as well (since in this case, the highest orbital moment does not lie at any charge value in the easy axis as it always points out of plane). Experimental evidence along with second-order perturbation theory and first principles calculations [38] suggest that Bruno's formula is a special case valid for systems when only the on-site contributions to the MA are taken into account and the exchange splitting is large enough. Apart from that, if the hybridizations become important and the spin-flip terms do not vanish, as in the case of strong SOCs (e.g., Au/Co/Au), a more general relationship between the MA and the OMA, which considers all the atomic species and off-site spin-orbit terms, needs to be employed [38]. Even more, the formalism was developed in the framework of neutral systems; therefore, no simple link between MA and OMA can be expected for systems with an excess of charge. Since Bruno's relation seems to be partially fulfilled for such systems, it is interesting to explore its limits by investigating the relationship between the MA and the OMA as a function of charge doping. Taking $Pt/Fe_2/Pt(100)$ as an example (illustrated in Fig. 4), one finds that the linear dependence is preserved for positive charging while stronger deviations to this linear behavior are observed at high charge density concentrations ($\sim 1e$/unit cell). From these results, one infers that the electronic environment significantly changes beyond a certain charge threshold, enhancing the hybridizations and the spin-orbit coupling between the Fe 3d and Pt 5d orbitals. When SOC is strong enough or when the hybridizations are dominant, even at moderate charge concentrations, no direct relationship between the MA and the OMA is observed. This assumption is clearer in the case of $Pt_2/Fe_2/Pt(100)$, when the two capped Pt layers boost the spin-orbit coupling leading to a nonlinear correspondence between the MA and the OMA. The interplay between the SOC strength and d-d hybridizations will determine the magnitude of the MA and the direction of magnetization at

once and hence whether or not Bruno's formula can be used. In our calculations we model the Fe-Pt multilayers by a slab in vacuum splitting the charge over both faces of the slab. Nevertheless, due to the strong effects that cause the charge doping, one would not expect significant changes in the trends and main conclusions discussed in the present work.

Summarizing, we have studied the surface-charging effects on the MA in 3d-5d layered alloys by using Fe-Pt multilayers as a particular model system. Surface charging results in direct consequences in both the magnitude and the direction of magnetization. A remarkable enhancement in the MA upon charge doping is found in Pt/Fe/Pt(100) and explained qualitatively in terms of second-order perturbation theory. In capped multilayers with double Fe layers, a spin reorientation occurs due to an enhancement of the hybridization caused by both alloying and charge doping. The large spin-orbit coupling of the nonmagnetic layers plays an essential role in determining the MA. Moreover, these interactions can be tuned by charge doping. Finally, Bruno's relation seems to be valid, to a large extent, for charged systems exhibiting strong hybridizations but moderate SOC interactions. In conclusion, we have demonstrated that charge doping may modify the magnetic properties of metallic multilayers and thus, it can be used as a promising technique for engineering novel materials with potential technological implications since by controlling the charge carrier density (charge doping), which can be mediated using the tip of a scanning probe microscope, the spin direction of the multilayers sample can be tailored either to have a perpendicular or parallel easy axis.

[1] C. G. Duan, S. S. Jaswal, and E. Y. Tsymbal, Phys. Rev. Lett. **97**, 047201 (2006).

[2] J. M. Rondinelli, M. Stengel, and N. Spalding, Science **315**, 349 (2007).

[3] X. Chen, A. Hochstrat, P. Borisov, and W. Kleeman, Appl. Phys. Lett. **89**, 202508 (2006).

[4] A. Lehnert, S. Dennler, P. Błoński, S. Rusponi, M. Etzkorn, G. Moulas, P. Bencok, P. Gambardella, H. Brune, and J. Hafner, Phys. Rev. B **82**, 094409 (2010).

[5] W.-G. Wang, M. Li, S. Hageman, and C. L. Chien, Nat. Mater. **11**, 64 (2011).

[6] J. Hu and R. Wu, Phys. Rev. Lett. **110**, 097202 (2013).

[7] M. Weisheit, S. Fähler, A. Marty, Y. Souche, C. Poinsignon, and D. Givord, Science **315**, 349 (2007).

[8] H. Gleiter, J. Wissmüller, O. Wollersheim, and R. Würschum, Acta Mater. **49**, 737 (2001).

[9] S. Schnur and A. Groβ, Catal. Today **165**, 129 (2011).

[10] G. Moulas, A. Lehnert, S. Rusponi, J. Zabloudil, C. Etz, S. Ouazi, M. Etzkorn, P. Bencok, P. Gambardella, P. Weinberger, and H. Brune, Phys. Rev. B **78**, 214424 (2008).

[11] J. Dorantes-Dávila, H. Dreyssé, and G. M. Pastor, Phys. Rev. Lett. **91**, 197206 (2003).

[12] M. Munoz-Navia, J. Dorantes-Dávila, D. Zitoun, C. Amiens, N. Jaouen, A. Rogalev, M. Respaud, and G. M. Pastor, Appl. Phys. Lett. **95**, 233107 (2009).

[13] M. Tsujikawa and T. Oda, Phys. Rev. Lett. **102**, 247203 (2009).

[14] S. Haraguchi, M. Tsujikawa, J. Gotou, and T. Oda, J. Phys. D **44**, 064005 (2011); M. Tsujikawa, S. Haraguchi, T. Oda, Y. Miura, and M. Shirai, J. Appl. Phys. **109**, 07C107 (2011).

[15] C. G. Duan, J. P. Velev, R. F. Sabirianov, Z. Zhu, J. Chu, S. S. Jaswal, and E. Y. Tsymbal, Phys. Rev. Lett. **101**, 137201 (2008).

[16] N. N. Negulyaev, V. S. Stepanyuk, W. Hergert, and J. Kirschner, Phys. Rev. Lett. **106**, 037202 (2011); T. R. Dasa, P. A. Ignatiev, and V. S. Stepanyuk, Phys. Rev. B **85**, 205447 (2012).

[17] C. Si, W. Duan, Z. Liu, and F. Liu, Phys. Rev. Lett. **109**, 226802 (2012).

[18] G. Shull, Y. J. Dappe, C. Gonzalez, H. Bulou, and R. Berndt, Nano Lett. **11**, 3142 (2011).

[19] T. Bazhirov and M. L. Cohen, J. Phys. Condens. Matter **25**, 105506 (2013).

[20] S. J. Gong, C.-G. Duan, Z.-Q. Zhu, and J.-H. Chu, Appl. Phys. Lett. **100**, 122410 (2012).

[21] S. Aihara, H. Kageshima, T. Sakai, and T. Sato, J. Appl. Phys. **112**, 073910 (2012).

[22] J. Repp, G. Meyer, F. E. Olsson, and M. Persson, Science **305**, 493 (2004).

[23] Y. Shen, S. Guo, J. Hu, and Y. Zhang, Appl. Phys. Lett. **101**, 183109 (2012).

[24] M. Zdrojek1, T. Mélin, C. Boyaval, D. Stiévenard, B. Jouault, M. Wozniak, A. Huczko, W. Gebicki, and L. Adamowicz, Appl. Phys. Lett. **86**, 213114 (2005).

[25] C. Liu and S. D. Bade, J. Vac. Sci. Technol. A **8**, 2727 (1990).

[26] P. Hohenberg and W. Kohn, Phys. Rev. **136**, B864 (1964); W. Kohn and L. J. Sham, Phys. Rev. **140**, A1133 (1965).

[27] G. Kresse and J. Hafner, Phys. Rev. B **47**, 558 (1993); G. Kresse and J. Furthmüller, Phys. Rev. B **54**, 11 169 (1996); http://cms.mpi.univie.ac.at/vasp.

[28] D. M. Ceperley and B. J. Alder, Phys. Rev. Lett. **45**, 566 (1980).

[29] J. P. Perdew and A. Zunger, Phys. Rev. B **23**, 5048 (1981).

[30] The energy cutoff for the plane-wave basis set was 400 eV, and the k-mesh size was $21 \times 21 \times 1$ ($29 \times 29 \times 1$) for the structural relaxations (relativistic calculations). Spin-orbit coupling is taken into account in the relativistic calculations. Geometric, electronic, and magnetic degrees of freedom are relaxed simultaneously until the forces acting on the atoms become less than 10^{-2} eV/Å and the changes in the total energy between two successive electronic steps are smaller than 10^{-7} eV, yielding an estimated error in energy less than 1 meV/atom.

[31] Strictly, the highest concentration of charge (holes) is placed in both sides (surfaces) of the slab with very small charge (holes) oscillations inside due to the relative reduced atomic thickness, but as the thickness of the slab is increased the excess of charge will lie only in the surface and the usual metalliclike behavior is then recovered.

[32] G. Makov and M. C. Payne, Phys. Rev. B **51**, 4014 (1995).

[33] For charged systems having a large dipolar moment, quadrupolar corrections to the total energy need to be considered over dipolar ones [32]. The corrected energy has the form $E(\vec{m}, q, Q) = E(\vec{m}, q) + \Delta E_{\mathrm{corr}}(q, Q)$ where $\vec{m}$, q, and Q are the magnetization, the excess of charge, and the quadrupolar moment, respectively. Assuming a scalar quadrupolar moment, $\Delta E_{\mathrm{corr}}(q, Q)$ is independent of the direction of magnetization; hence, the MA is independent of the quadrupolar corrections, i.e., MA = $E(m_\perp, q, Q) - E(m_\parallel, q, Q)$.

[34] P. Bruno, Phys. Rev. B **39**, 865 (1989).

[35] The linear dependence in the MA has already been observed for the same sample in the presence of an EEF but never achieves the large values found in this study through charge doping. Its origin is often attributed to the small variations of the number of the valence electrons near the Fermi level induced by the EEF [7,13].

[36] D. S. Wang, R. Wu, and A. J. Freeman, Phys. Rev. B **47**, 14932 (1993).

[37] M. Tsujikawa, A. Hosokawa, and T. Oda, Phys. Rev. B **77**, 054413 (2008).

[38] C. Andersson, B. Sanyal, O. Eriksson, L. Nordström, O. Karis, D. Arvanitis, T. Konishi, E. H. Krappe, and J. H. Dunn, Phys. Rev. Lett. **99**, 177207 (2007).